

## An Active Virtual Impedance Control Algorithm For Collision Free Navigation of a Mobile a Robot

Jinho Kim, Jangmyung Lee

Departement of Electrical and Electronic Engineering, Pusan National University, Jangjeon 2-dong, Geumjeong-gu, Busan 609-735, Republic of Korea

---

### Article Info

#### Article history:

Received Feb 7, 2017

Revised Apr 15, 2017

Accepted Apr 30, 2017

---

#### Keyword:

Microphone array

Mobile robot

Obstacle avoidance

Sound source

Virtual impedance,

---

### ABSTRACT

An modified active virtual impedance control has been proposed for collision free navigation of a mobile robot to avoid front obstacles dynamically while a mobile robot is following a sound source. A mobile robot is controlled to follow a sound source with a velocity which is determined by virtual repulsive and attraction forces to avoid obstacles and to follow the sound source, respectively. To generate the virtual repulsive and attraction forces, a new modified virtual impedance is defined as a function of the distances and relative velocities to the sound source and obstacles from the mobile robot. In the conventional virtual impedance method, fixed coefficients have been used for the virtual impedance control. In this research, the coefficients are dynamically adjusted to elaborate the obstacle avoidance performance in various situations such as the multiple moving obstacles environment. A microphone array consisting of three microphones in a row has been attached on the mobile robot to detect the relative distance and velocity to the obstacles. The relative position and orientation of the sound source against the mobile robot has been estimated using the geometrical relationship of the microphones. As an application, the mobile robot can be used as a pet robot following the master with a sound source. The effectiveness of the proposed algorithm has been demonstrated through real experiments.

Copyright © 2017 Institute of Advanced Engineering and Science.  
All rights reserved.

---

### Corresponding Author:

Jangmyung Lee,

Departement of Electrical and Electronic Engineering

Pusan National University,

Jangjeon 2-dong, Geumjeong-gu, Busan 609-735, Republic of Korea.

Email: jmlee@pusan.ac.kr

---

## 1. INTRODUCTION

A microphone array has been used to detect the location of a sound source, either a human or a sounding machine [1]. At each microphone, the sound wave arrives with a different phase and magnitude. Therefore, the geometric relationship among the microphones and the differences in the arrived sound signals can be used to estimate the location of the sound source. The magnitude of the sound signal arriving at the microphone is inversely proportional to the square of the distance from the microphone to the sound source. Normally, sound source detection for long distances is not feasible because the sound signal is so susceptible to environmental noise. The sound signal has reflection, diffraction, and interferences against the environment conditions, such as air temperature, existence of obstacles, size of the space, and surrounding sound signals which cause signal distortions and degrade the reliability of the signal.

TDOA (Time Difference of Arrival) algorithm has been adopted using an array of microphones, which are used to measure the arrival time difference. The time difference includes the phase difference and magnitude similarity among the sound signals received at the microphone array. The maximum and threshold values can be used to measure the similarity of the signals. However, the method is not robust against noises.

The difference and cross correlation or the generalized cross correlation method have been used for robust similarity measurements [1-6].

Recently, the sound source location has been estimated by mapping the cross-correlation function onto a geometrical space, instead of estimating the time difference for the functions [4-6]. The HRTF (Head Related Transfer Function), a beam forming method, and artificial ear method are used to detect the sound source location for robots. Most of them require heavy computations and are expensive when applied to robotic applications [6-12]. Because recognition of the sound source location is quite susceptible to noise, recognition research has focused on specific signals. Currently with the developments of system technology, the recognition of the sound source has become feasible when applied to real applications. The recognition of a sound source is useful for navigating mobile robots to follow a sound source or avoid obstacles [13-14]. For the sound source following robot, a sudden change in the angles and a very high speed motion might be needed to follow the arbitrary sound source. Following the sound source and avoiding obstacles, the relationship among the recognized sound source and the mobile robot is very important and needs to be maintained properly. The location of the mobile robot is identified by the dead reckoning method using an encoder. Obstacles exist in the moving path, which should be avoided with a suitable sensor during the following operation.

Several studies have examined real time obstacle avoidance, such as VFH (Vector Field Histogram approach), CVM (Curvature Velocity Method), and DWA (Dynamic Window Approach), which have local minima to be avoided with certain modifications [15-17]. The PFM (Potential Field Method) has been proposed to generate an attraction force to the target and a repulsive force against an obstacle to determine the direction and velocity of the mobile robot [16-18].

In this study, the virtual impedance method has been adopted and elaborated to improve the obstacle avoidance performance [18]. The relationship between the uncertain environment and the mobile robot has been modeled as an impedance formed by the damper and spring, which generates a potential vector for the mobile robot [19-22]. The conventional virtual impedance algorithm may confront with a local minimum during navigation by the obstacles with fixed coefficients of the impedance. In this study, the impedance has been adjusted dynamically to improve the collision avoidance performance, and the scheme is called the active virtual impedance method. The location of the sound source has been estimated based on the TDOA and using the cross-correlation algorithm; the virtual impedance algorithm has been applied to allow a mobile robot to follow a sound and avoid obstacles.

This paper consists of six sections including this introduction. The location estimation of the sound source is discussed in Section 2. As a key idea of this paper, the active virtual impedance algorithm has been derived in Section 3, the experimental systems of the mobile robot and sensors are illustrated in Section 4, and the experimental results are discussed in Section 5. Finally, Section 6 concludes this research and proposes future research.

## 2. LOCALIZATION OF SOUND SOURCE

### 2.1. Point sound source

An artificial sound can be generated with a regular pattern using a speaker or a vibrating motor to be used for localization. The point source generated in a short period radiates short term energy, which can be recognized easily. The frequency of sound,  $f$ , traveling with the velocity  $v$  can be changed to  $f'$  by the relative velocity at the receiver point using the Doppler formula as follows (1):

$$f' = f \left( \frac{c \pm v_c}{c \pm v_s} \right) \quad (1)$$

where  $v_c$  and  $v_s$  represent the velocity of the receiver and sound source, respectively.  $c$  is the propagation velocity of the sound. The Doppler effect can be ignored when  $c \gg v_c$  and  $c \gg v_s$  *i.e.* the velocities of the sound source and the mobile robot are considerably smaller than the propagation velocity of sound. Diffusion, diffraction, and reflection of the sound signal in the environment make the signal recognition for the localization difficult.

The sound signal velocity,  $c$ , is 340 m/s in the air at room temperature. Using this velocity and traveling time, the distance between the sound source and microphone can be calculated.

## 2.2. Arriving time difference method

The distance from the sound source to  $i_{th}$  microphone,  $R_i$ , can be obtained as follows (2):

$$R_i [m] = t_i [s] \times c [m/s], \quad i = 1, 2, 3 \quad (2)$$

where  $t_i$  is the traveling time of the sound source to the  $i_{th}$  microphone. When there are two neighboring receivers, the received signals can be represented as,  $x_1(n)$  and  $x_2(n)$  for  $k=0$  to  $n$  sampling moments, respectively. The similarity function,  $S_{x_1, x_2}$ , can be defined from these two data sets as follows (3):

$$S_{x_1, x_2} = 1 / \sum_{k=0}^{n-1} \sqrt{(x_1(k) - x_2(k))^2} \quad (3)$$

When the signal  $x_j(k)$  is shifted  $n$  steps, the maximum similarity function can be represented as (4):

$$S_{x_i, x_j}(j_M) = 1 / \sum_{k=0}^{n-1} \sqrt{(x_i(k) - x_j(k + j_M))^2} \quad (4)$$

where  $j_M$  is  $0 \sim n-1$ . Using Eq. (4),  $j_M$ , which gives the maximum similarity value, can be obtained. The arrival time difference between the two microphones,  $\Delta t_{ij}$ , can be calculated using  $j_M$  and the sampling period, which is represented as (5):

$$\Delta t_{ij} = j_M \times t_{sampling} \quad (5)$$

where  $t_{sampling}$  represents the sampling period of the data sets.

## 2.3. Recognition of sound source

For the simplicity of obtaining the distances,  $R_i$ , and angles,  $\theta_i$  to the sound source, three microphones,  $M_1$ ,  $M_2$ , and  $M_3$  are installed on the same plane with a constant interval ( $l = 40 \text{ Cm}$ ). In Figure 1, the distances to the microphones,  $M_1$ ,  $M_2$ , and  $M_3$ , from the sound source are represented as  $R_1$ ,  $R_2$ , and  $R_3$ , respectively. And the  $D$  is a normal distance to the sound source from the microphones. The  $t$  ( $i = 1, 2, 3$ ) can be defined as the traveling time of the sound source to the  $i^{th}$  microphone, which also defines  $\Delta t_{12}$  and  $\Delta t_{13}$  as the arrival time difference between two microphones, 1-2 and 1-3, respectively.

From Figure 1, the distance to the sound source,  $D$ , can be obtained using the triangular area formula. Using the Heron's formula, the areas of two triangles,  $\Delta SM_1M_2$  and  $\Delta SM_2M_3$ , can be obtained as follows:

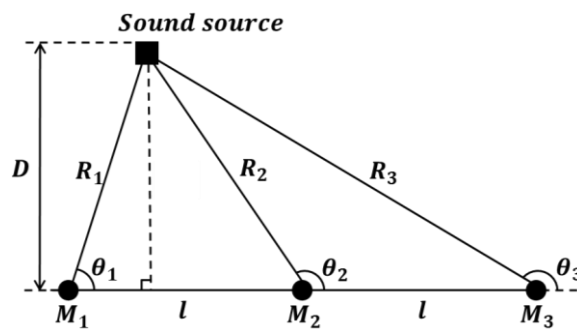


Figure 1. Geometrical structure of the microphones and a sound source in 2D space.

From Figure 1, the distance to the sound source,  $D$ , can be obtained using the triangular area formula. Using the Heron's formula, the areas of two triangles,  $\Delta SM_1M_2$  and  $\Delta SM_2M_3$ , can be obtained as follows (6-7):

$$\Delta SM_1M_2 = \sqrt{s_1(s_1 - R_1)(s_1 - R_2)(s_1 - l)} \quad (6)$$

$$\Delta SM_2M_3 = \sqrt{s_2(s_2 - R_2)(s_2 - R_3)(s_2 - l)} \quad (7)$$

where  $s_1 = \frac{1}{2}(R_1 + R_2 + l)$  and  $s_2 = \frac{1}{2}(R_2 + R_3 + l)$ .

The two areas are actually the same. By placing this relation into Equation (6), (7), the distance  $D$  can be obtained as follows (8):

$$D = \frac{2l^2 + c^2(\Delta t_1^2 + 2\Delta t_2^2 - \Delta t_3^2)}{2c(\Delta t_1 - 2\Delta t_2 + \Delta t_3)}. \quad (8)$$

Using the cosine laws, the orientation angle,  $\theta$ , can be estimated when the arrival time differences,  $\Delta t_i$ , are available. The arrival angle of the sound signal can be calculated as follows (9-11):

$$\theta_1 = \sin^{-1}\left(\frac{D}{D + c \cdot \Delta t_1}\right) \quad (9)$$

$$\theta_2 = \pi - \sin^{-1}\left(\frac{D}{D + c \cdot \Delta t_2}\right) \quad (10)$$

$$\theta_3 = \pi - \sin^{-1}\left(\frac{D + c \cdot \Delta t_2}{D + c \cdot \Delta t_3}\right) \quad (11)$$

### 3. Active virtual impedance

To avoid obstacles more efficiently by the navigation robot, a new active virtual impedance algorithm has been proposed.

#### 3.1. Collision vector

To avoid the obstacles during the navigation of a mobile robot, the locations of the obstacles need to be identified first. The distance vector from the sensor to an obstacle,  $\vec{L}_i$  ( $i$ : integer) can be defined as (12):

$$\vec{L}_i = (x_i, y_i) - (r_i \cos \theta_i, r_i \sin \theta_i) \quad (12)$$

where  $r_i$  represents the distance to an obstacle from the  $i^{\text{th}}$  sensor;  $\theta_i$  represents the angle between the robot moving direction  $Y_R$  and  $i^{\text{th}}$  sensor and  $(x_i, y_i)$  represent the location of the  $i^{\text{th}}$  sensor.

To detect obstacles in front of the mobile robot, three distance sensors are attached in front of the mobile robot. A collision vector,  $\vec{C}$  is defined using the sense data. Two different situations occur when defining the collision vector. Case 1: When the obstacle is small, it can be detected only by a distance sensor. In this case, the collision vector,  $\vec{C}$  is defined as (13):

$$\vec{C} = \vec{L} \quad (13)$$

Case 2: When the obstacle is detected by two distance sensors, the collision vector,  $\vec{C}$  can be defined using two pointing vectors,  $\vec{L}_i$  and  $\vec{L}_{i+1}$ . From the two pointing vectors, as shown in Figure 2, two obstacle points  $P_i$  and  $P_{i+1}$  can be obtained as follows (14):

$$P_i = (r_i \cos \theta_i, r_i \sin \theta_i) \quad (14-a)$$

$$P_{i+1} = (r_{i+1} \cos \theta_{i+1}, r_{i+1} \sin \theta_{i+1}) \quad (14-b)$$

The line between the two points,  $P_i$  and  $P_{i+1}$  can be obtained and represented as  $\overline{P_i P_{i+1}}$ . Then a collision vector from the mobile robot to an obstacle can be defined as  $\overline{P_0 P_c}$ , which is vertical to the line  $\overline{P_i P_{i+1}}$  from the origin of the mobile robot,  $P_0$ . Now the collision vector *w.r.t.* the robot frame,  ${}^R\vec{C}_c$ , is defined as follows (15):

$${}^R\vec{C}_c = \begin{bmatrix} \frac{m \cdot x_i - y_i}{m + \frac{1}{m}} & \frac{-m \cdot x_i + y_i}{m^2 + 1} \\ \frac{1}{m} & m^2 + 1 \end{bmatrix}^T \quad (15)$$

where  $m = \frac{y_{i+1} - y_i}{x_{i+1} - x_i}$  and  $P_0$  is defined as the origin of the mobile robot *w.r.t.* a world frame.

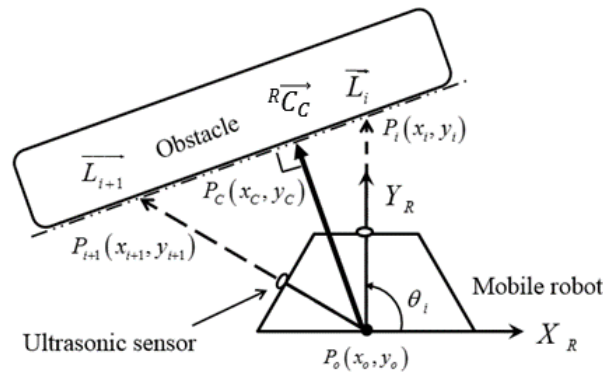


Figure 2. Definition of a Collision vector

The driving vector is defined *w.r.t.* the mobile robot frame, which needs to be transformed to a world frame to drive the mobile robot to a target position specified *w.r.t.* the world frame. Space rotation of the driving vector as shown in Figure 3.

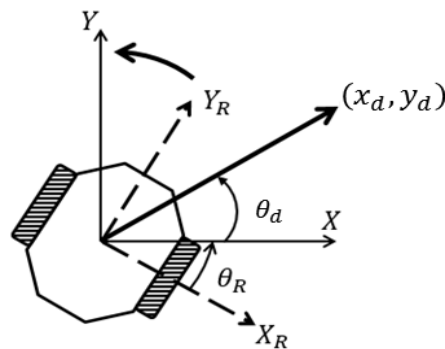


Figure 3. Space rotation of the driving vector.

As shown in Figure 3, the orientation of the mobile robot can be transformed to the world frame by rotating  $\theta_R$  along the  $z$ -axis as follows (16):

$$\begin{bmatrix} x_w \\ y_w \\ \theta_w \end{bmatrix} = \begin{bmatrix} \cos \theta_R & \sin \theta_R & 0 \\ -\sin \theta_R & \cos \theta_R & 0 \\ 0 & 0 & 1 \end{bmatrix} \begin{bmatrix} x_d \\ y_d \\ \theta_d \end{bmatrix} \quad (16)$$

Therefore, the driving vector can be represented *w.r.t.* the world frame as follows (17):

$${}^w\vec{C} = [x_0 + x_d \quad y_0 + y_d]^T \quad (17)$$

### 3.2. Virtual impedance model

The relative distance and velocity between the mobile robot and an obstacle can be modeled as a spring and damper, respectively, which is called the virtual impedance. Using this virtual impedance, the acceleration for the mobile robot to avoid the obstacle,  $\ddot{X}_s$ , can be defined.

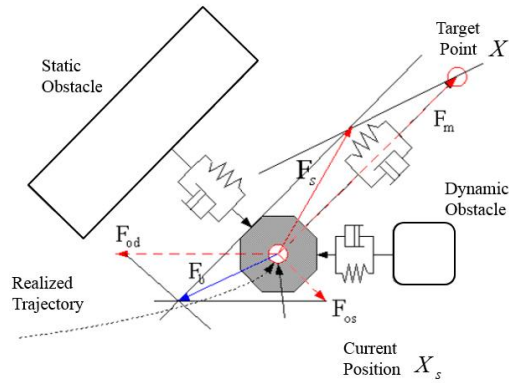


Figure 4. Virtual impedance model

From the virtual impedance model illustrated in Figure 4, the acceleration equation of the mobile robot can be obtained as follows (18):

$$\ddot{x}_s = \frac{1}{M_s} \left( F_m + \sum_{i=1}^{n_{os}} F_{os,i} + \sum_{i=1}^{n_{od}} F_{od,i} \right) \quad (18)$$

where  $F_m$  represents the attraction force to the target point,  $X_r$ ;  $M_s$  represents the mass of the mobile robot;  $\ddot{x}_s$  represents the acceleration of the mobile robot;  $F_{os,i}$  and  $F_{od,i}$  are the repulsive forces against the  $i^{\text{th}}$  static and dynamic obstacles, respectively;  $n_{os}$  and  $n_{od}$  represent the number of static and dynamic obstacles, respectively.

The addition of the three forces,  $F_m$ ,  $F_{os}$  and  $F_{od}$ , guides the mobile robot to the target while avoiding the obstacles. The forces are described in detail as follows (19):

$$F_s = F_m + F_{os} + F_{od} \quad (19)$$

where  $F_m = K_r(X_r - X_s) + D_r(-\dot{X}_s)$ ,  $F_{os} = \sum_{i=1}^{n_{os}} \{K_{s,i}(X_s - x_{s,i}) + D_{s,i}(\dot{X}_s - \dot{x}_{s,i})\}$  and

$$F_{od} = \sum_{i=0}^{n_{od}} \{K_{d,i}(X_s - x_{d,i}) + D_{d,i}(\dot{X}_s - \dot{x}_{d,i})\}.$$

Note that  $x_{s,i}$  and  $x_{d,i}$  represent the position of the  $i^{th}$  static and dynamics obstacles, respectively. The variables in Equation (19) are summarized in Table 1.

Table 1. Constants for virtual impedance algorithm.

Variable	Definition
$K_r$	Spring constant to target position
$D_r$	Damping constant to target position
$K_{s,i}$	Spring constant for $i_{th}$ static obstacle
$D_{s,i}$	Damping constant for $i_{th}$ static obstacle
$K_{d,i}$	Spring constant for $i_{th}$ dynamic obstacle
$D_{d,i}$	Damping constant for $i_{th}$ dynamic obstacle

The repulsive force  $F_b (= F_{os} + F_{od})$  can be represented using the obtained collision vector  ${}^W\vec{C}$  w.r.t. the world frame as follows:

$$F_b = K_o \left\| {}^W\vec{C} \right\|^{-1} \bar{u}_c + D_o \left\| \frac{d}{dt} {}^W\vec{C} \right\| \bar{u}_c \quad (20)$$

where  $K_o$  is a spring coefficient,  $D_o$  is a damping coefficient, and  $\bar{u}_c = -{}^W\vec{C} \cdot \left\| {}^W\vec{C} \right\|^{-1}$ . The repulsive force is generated regardless of the types of obstacles and all the repulsive forces are added together.

For the static obstacle, the conventional virtual impedance algorithm is effective. On the other hand, when there are multiple obstacles, the mobile robot is jammed and cannot navigate further. In addition, the sudden repulsive force against the moving obstacle causes unstable velocity changes to the mobile robot so that the mobile robot vibrates on the path or deviates from the path. Flowchart of the sound source tracking mobile robot system as shown in Figure 5.

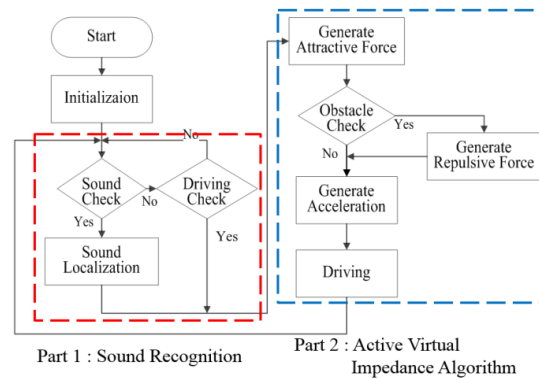


Figure 5. Flowchart of the sound source tracking mobile robot system.

### 3.3. Active virtual impedance algorithm

A new active virtual impedance algorithm is proposed to overcome the disadvantages of the conventional virtual impedance method[22] that generates attractive and repulsive forces proportional to the distance and relative velocities against the target and obstacle. Because the collision possibility increases abruptly when the obstacle approaches the mobile robot with a high relative velocity, a new nonlinear active virtual impedance has been proposed to incorporate the situations as follows (21):

$$F_b = K_a \left\| {}^w \bar{C} \right\|^{-1} \bar{u}_c + D_a \left\| \frac{d}{dt} {}^w \bar{C} \right\| \bar{u}_c \quad (21)$$

where  $K_a$  and  $D_a$  are defined as Figure 5(a) and (b), respectively.

Figure 6 shows  $K_a$  and  $D_a$  as a function of the distance and relative velocity against the obstacle, which are in Equation (21). As shown in Figure 6(a), the  $K_a$  increases when the distance to the obstacle decreases until  $\rho_1$ . However, when the distance is very small, the repulsive force needs to be saturated to consider the maximum velocity of the mobile robot to avoid the obstacle. Therefore the  $K_a$  value is set to be decreased when the distance is smaller than  $\rho_1$ . On the other hand, the repulsive force against the relative velocity is considered effective below,  $\mu_1$ , as shown in Figure 6(b). Note that when the relative velocity to the obstacle is larger than,  $\mu_1$ , the gain,  $D_a$ , is adjusted not to require the maximum velocity of the mobile robot.

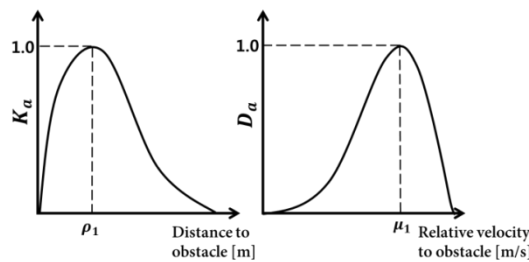


Figure 6. Determination of  $K_a$  and  $D_a$

## 4. Experimental systems

### 4.1. Mobile robot

For this study, two differential-driving mobile robots are developed. A front robot generates sound signals while it is traveling. The rear robot follows the sound source according to the acceleration generated by the active virtual impedance algorithm as shown in Equation. (18). Figure 7 shows the sound source mobile robot system. To help the sound recognition, the front robot generates a sound signal for 0.5 s in every 2 s.

Sound source: The mobile robot in Figure 7 is designed to carry the sound source, NT-Commander-1 generated by NTRexLAB. Two DC motors are RB-35GM produced by D&J WITH, which have 50:1 reduction gears and encoders (2,600 pulses/rot). To amplify the sound signal, the R002(5 W) power amplifier by FunnyKIT Corp. has been used with a LS-705(30 W) speaker produced by Lotte Electronics Corp. Table II summarizes the hardware specifications of the moving sound source.



Figure 7. Moving sound source.

Table 2. Hardware specifications of the moving object

List	Specification
Size(mm)	352(W)*326(L)*320(H)
Weight(kg)	5.3
Distance between wheels(mm)	290
Radius of wheel(mm)	60

**Mobile robot:** The differential-driving mobile robot in Figure 8 is designed using two DC IG-32PGM motors for each wheel and a ball caster to balance the system. The reduction gears with a 50:1 reduction ratio have been used for motors with encoders (2,600 pulses/rot). A microphone array has been formed using three microphones of ETM-001, which has -23 dB omni-directional sensitivity for 50 Hz to 18 kHz signals. The distance between the microphones is 40 cm. The received signal is amplified by K2372 (universal stereo pre-amplifier kit, Velleman Corp.) to 40 dB. An ARM series MyCortex-LM 8962 is used as an MCU and the signal is sampled by 100 kHz and has been converted to a digital signal using a 10-bit ADC. Table III summarizes the hardware specifications of the mobile robot.

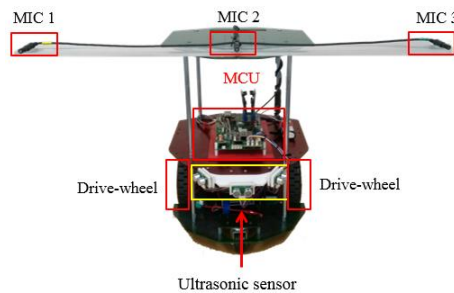


Figure 8. Components of the experimental mobile robot.

Table 3. Hardware specifications of the mobile robot.

List	Specification
Size(mm)	350(W)*820(L)*262(H)
Weight(kg)	3.94
Distance between wheels(mm)	410
Radius of wheel(mm)	60

#### 4.2. Sensors and estimation of distances to obstacles

To detect the obstacles, an ultrasonic sensor SRF-05, which is cheap and easy to use has been utilized. The detection angle is limited by  $30^\circ$  within the range of 3~300 cm. To overcome the narrow detecting angle of the ultrasonic sensor, three ultrasonic sensors are installed on the mobile robot to follow the sound source while it is avoiding obstacles, as shown in Figure 9.

The performance of obstacle avoidance is determined by the sensors to detect obstacles and control algorithms to avoid the obstacles. Therefore, the characteristics of the sensors should be considered carefully for obstacle avoidance. The ultrasonic sensor, SRF-05, radiates a 40 kHz signal, whose propagation velocity depends on the material of the path and the temperature of the material.

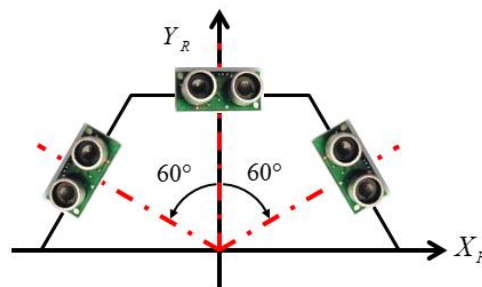


Figure 9. Configuration of the ultrasonic sensors on the mobile robot.

Notice that the TOF (Time of Flight) of the ultrasonic signal is dependent on the velocity which is represented as (22):

$$v [m/sec] = 331.5 + 0.6 \times T \quad (22)$$

where  $T$  is the temperature in Celsius.

## 5. EXPERIMENTS

To test the superiority of the proposed algorithm, three experiments have been performed. Experiment 2: Avoidance of multiple static obstacles. The active virtual impedance algorithm has been applied to the mobile robot navigation under a static obstacle environment as shown in Figure 11, where two obstacles are located in the path to the goal position where the sound source is located

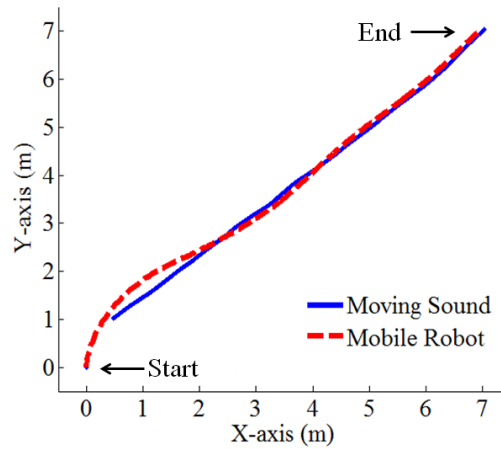


Figure 10. Experiments for checking the performance of sound tracking.

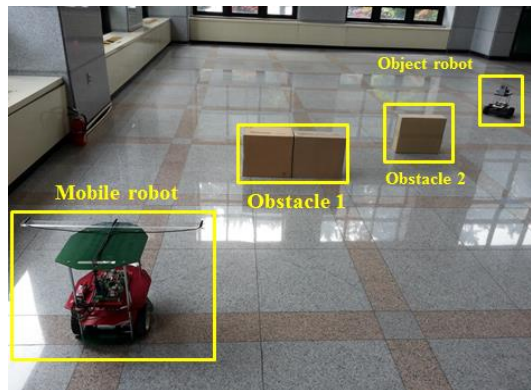


Figure 11. Experimental environment for multiple fixed obstacle avoidance. (The size of obstacles are 100 (W) \* 30 (H) \* 50 (D) mm for Obstacle 1 and 80 (W) \* 30 (H) \* 50 (D) mm for Obstacle 2)

Figure 12 compares the experimental trajectories using the conventional virtual impedance algorithm and the new active virtual impedance algorithm. The threshold value,  $\rho_1$ , is selected as 100 mm not to over-drive the mobile robot when the obstacle is very near to the robot. Notice that the repulsive force for the distance to the obstacle is nonlinear as shown in Figure 6(a) in this active virtual impedance algorithm. Also  $\mu_1$  is selected empirically to keep the maximum velocity of the mobile robot smaller than 720 mm/s.

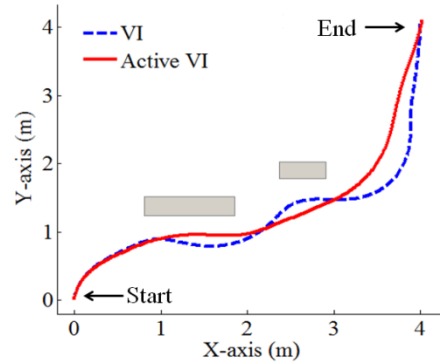


Figure 12. Experimental results of collision free navigation with multiple fixed obstacles.

As shown in Figure 12, the trajectory of the mobile robot by the active virtual impedance algorithm is smoother than that by the conventional algorithm. This is the effect of the active virtual impedance, which detects long distance obstacles and gradually changes the trajectory of the mobile robot earlier without causing a high speed motion of the mobile robot. Using this smooth trajectory, the mobile robot can reduce the slippage on the path, *i.e.* it can increase the trajectory accurately during multiple obstacles avoidance.

#### Experiment 3: Avoidance of dynamic obstacles

The active virtual impedance algorithm has been applied to dynamic obstacle avoidance for single and multiple obstacles [22].

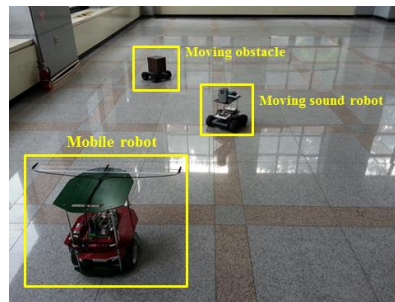
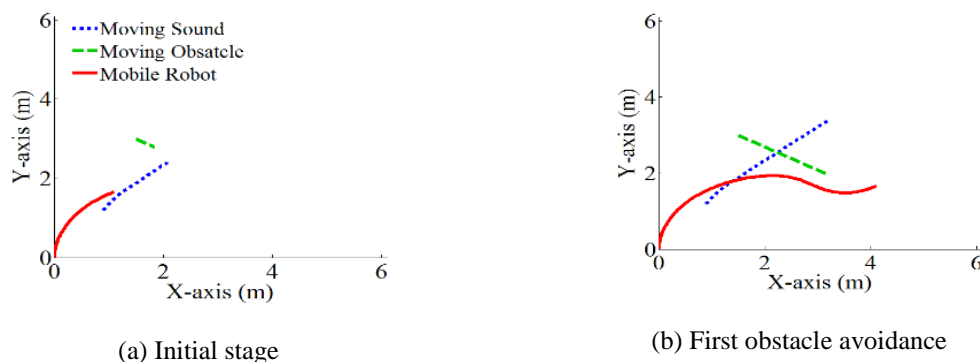


Figure 13. Experimental environment for moving obstacle avoidance (The size of moving obstacle is 80 (W) \* 30 (H) \* 50 (D) mm)

Figure 13 shows the experimental environment of dynamic obstacle avoidance. The space is 6.0 m wide and 8.0 m long. The sound source is moving with a velocity of 300 mm/s and  $\mu_0$  is set to keep the velocity of the mobile robot below 720 mm/s which is the maximum velocity of the mobile robot. Notice that the moving sound robot carries the sound source on the top of the robot.



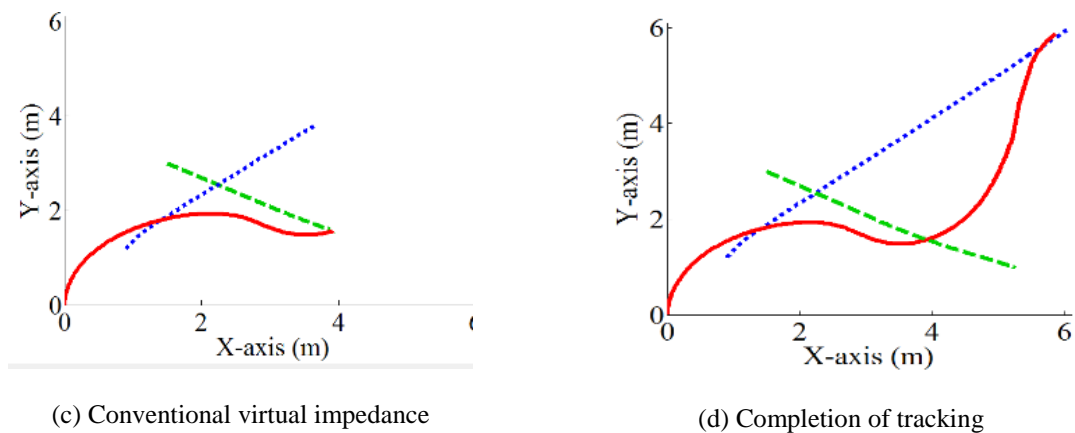


Figure 14. (a), (b) and (d) demonstrate the successful tracking of the sound source by the mobile robot using the active virtual impedance; (c) shows the collision situation when the conventional virtual impedance algorithm has been used for the tracking.

Figure 14 shows the experimental results of the dynamic obstacle avoidance. As demonstrated in the sequence, the mobile robot successfully follows the sound source while it is avoiding the moving obstacle. As shown in Figure 14(c), the mobile robot collides with the obstacle when the conventional virtual impedance algorithm has been utilized to avoid a collision. However, a fast-repulsive force is generated by the active virtual impedance which enables the mobile robot to avoid the collision. Figure 14(d) illustrates the successful tracking of the sound source by the mobile robot while it is avoiding the two moving obstacles.

## 6. CONCLUSION

This paper proposed an active virtual impedance algorithm for obstacle avoidance and for following sound sources in real time using a mobile robot. The active virtual impedance algorithm changes the impedance dynamically depending on the possibility of collision to the obstacle, which makes obstacle avoidance more efficient than the conventional virtual impedance algorithm. Before the mobile robot is approaching the obstacles, the motion trajectory of the mobile robot needs to be modified to prevent abrupt changes in the path, which may cause slippage of the mobile robot. The microphone array has been used to detect the location of the sound source, which is also a critical factor for successful sound source tracking. When there are multiple dynamic obstacles in various directions of the working environment, more ultrasonic sensors are necessary for the mobile robot to avoid the collisions, which is left for a future research work.

## ACKNOWLEDGEMENTS

This research was supported by the MOTIE (Ministry of Trade, Industry & Energy), Korea, under the Industry Convergence Liaison Robotics Creative Graduates Education Program supervised by the KIAT (N0001126)

## REFERENCES

- [1] K. Koderu, *et al.*, "Sound Localization of Approaching Vehicles Using Uniform Microphone Array," *Proc. IEEE Intelligent Transportation Systems Conference*, pp. 1054-1058, Oct 2007.
- [2] Q. Xu, *et al.*, "Sound source localization system based on mobile robot," *Chinese Control and Decision Conference (CCDC), 2012 24th Chinese*. May 2012.
- [3] X. Li, *et al.*, "Real-time sound source localization for a mobile robot based on the guided spectral-temporal position method," *International Journal of Advanced Robotic Systems*, no. 9, pp. 1-8, Sep 2012.
- [4] J. H. Han, *et al.*, "The Tracking of a Moving Object by a Mobile Robot Following the Object's Sound," *Journal of intelligent & robotic systems*, vol. 71, no. 1, pp. 31-42, Jul 2013.
- [5] J. S. Hu, *et al.*, "Simultaneous Localization of a Mobile Robot and Multiple Sound Sources Using a Microphone Array," *Advanced Robotics*, vol. 25, no. 1-2, pp. 135-152, Apr 2011.
- [6] K. C. Kwak, "Sound source tracking of moving speaker using multi-channel microphones in robot environments," *Proceeding of the 2011 IEEE International Conference on Robotics and Biomimetics*, pp. 3017-3020, Dec 2011.

- [7] Y. K. Shin, *et al.*, "Human Postural Dynamics in Response to the Horizontal Vibration," *International Journal of Control, Automation, and Systems*, vol. 4, no. 3, pp. 325-332, Jun 2006.
- [8] K. C., *et al.*, "Sound source localization with aid of excitation source information in home robot environment," *IEEE Trans on Consumer Electronics*, no. 54, pp. 852-856, May 2008.
- [9] J. M. Valin, *et al.*, "Robust localization and tracking of simultaneous moving sound sources using beamforming and particle filtering," *Robotics and Autonomous Systems*, vol. 55, no. 3, pp. 216-228, Mar 2007.
- [10] J. M. Valin, *et al.*, "Localization of simultaneous moving sound sources for mobile robot using a frequency-domain steered beamformer approach," *IEEE International Conference on ICRA*, pp. 1033-1038, Feb 2004.
- [11] V. Tourbabin, *et al.*, "Theoretical Framework for the Optimization of Microphone Array Configuration for Humanoid Robot Audition," *IEEE/ACM Transactions on Audio, Speech, and Language Processing*, vol. 22, no. 12, pp. 1803-1814, Dec 2014.
- [12] F. Keyrouz, "Advanced Binaural Sound Localization in 3-D for Humanoid Robots," *IEEE Transactions on Instrumentation and Measurement*, vol. 63, no. 9, Sept 2014.
- [13] P. Ratsamee, *et al.*, "Human-Robot collision avoidance using a modified social force model with body pose and face orientation," *International Journal of Humanoid Robotics*, vol. 10, no. 01, pp. 1350008(24 pages), Apr 2013.
- [14] P. Ögren, *et al.*, "A convergent dynamic window approach to obstacle avoidance," *IEEE Transactions on Robotics*, vol. 21, no. 2, pp. 188-195, Apr 2005.
- [15] Q. Zhang, *et al.*, "Dynamic obstacle-avoiding path planning for robots based on modified potential field method," *9th International Conference, ICIC 2013*, pp. 332-342, Jul 2013.
- [16] Iswanto, *et al.*, "Path Planning Based on Fuzzy Decision Trees and Potential Field," *International Journal of Electrical and Computer Engineering (IJECE)*, vol. 6, no. 1, pp. 212-222, Nov 2015.
- [17] L. Yin, *et al.*, "A new potential field method for mobile robot path planning in the dynamic environments," *Asian Journal of Control*, vol. 11, no. 2, pp. 214-225, Mar 2009.
- [18] S. I. A, *et al.*, "Simultaneous Task Assignment and Path Planning Using Mixed-Integer Linear Programming and Potential Field Method," *2013 13th International Conference on Control, Automation and Systems*, pp. 1845-1848, Oct 2013.
- [19] M. talezadeh, *et al.*, "The Mobile Robot HILARE: Dynamic Modeling and Motion Simulation," *International Journal of Robotics and Automation (IJRA)*, vol. 4, no. 2, pp. 150-155, May 2015.
- [20] R. Puviarasi, *et al.*, "Self Assistive Technology for Disabled People – Voice Controlled Wheel Chair and Home Automation System," *International Journal of Robotics and Automation (IJRA)*, vol. 2, no. 2, pp. 120-130, Dec 2014.
- [21] Y. W. Lee, *et al.*, "Distributed Unmanned Aircraft Collision Avoidance Using Limit Cycle," *2011 11th International Conference on Control, Automation and Systems*, vol. 3, no. 1, pp. 30-38, Jan 2014.
- [22] J. H. Han, *et al.*, "Obstacle avoidance of a moving sound following robot using active virtual impedance," *Journal of Institute of Control, Robotics and Systems*, vol. 20, no. 2, pp. 200-210, Feb 2014.

## BIOGRAPHIES OF AUTHORS



Jin-Ho Kim

received the B.S. degree in Electronic Engineering from Inje University, Gimhae, Korea, in 2015 and received M.S. degree in Electronic Engineering from Pusan National University, Busan, Korea, in 2017, e is currently working toward a Ph.D. degree in Electronic Engineering from Pusan National University, Busan, Korea. His research interests include Navigation/Localization, intelligent robot control and microprocessor application.



Prof. Jang-Myung Lee

received his B.S. degree and M.S. degree both in electronic engineering from Seoul National University, Seoul Korea, in 1980 and 1982, respectively, and received Ph.D. degree in computer engineering from the University of Southern California (USC), Los Angeles, in 1990. Since 1992, he has been a Professor with the Intelligent Robot laboratory, Pusan National University, Busan Korea. Dr. Lee is a former Chairman of the Research Center for Special Environment Navigation/Localization. He was president of the Korean Robotics Society in 2010. His current research interests include intelligent robotic systems, transport robot, and intelligent sensor and control algorithms.